J. Phys. D: Appl. Phys. **21** (1988) S28–S31/ECOOSA '88. Printed in the UK

Polarisation effects in weak localisation of light

M P van Albada†, M B van der Mark† and A Lagendijk†‡

† Natuurkundig Laboratorium der Universiteit van Amsterdam, Valckenierstraat 65, NL-1018 XE Amsterdam, The Netherlands
‡ FOM–Instituut voor Atoom- en Molecuulfysica, Kruislaan 407, NL-1098 SJ Amsterdam, The Netherlands

Received 3 May 1988

Abstract. Enhanced backscattering from a random medium resulting from interference is known as weak localisation. In the backscattered light three polarisation effects are observed: there is partial retention of polarisation, the polarised cone of enhanced backscattering is spatially anisotropic, and a slight enhancement is found in the depolarised light component. It is proved experimentally that the three effects are due to lower-order scattering contributions, and the effects are explained. A computer simulation of enhanced backscattering from a medium containing randomly distributed Rayleigh scatterers confirms this interpretation.

The phenomenon of enhanced backscattering has been known for a long time, and various explanations based upon geometrical optics are possible [1]. Recently, interference was proposed as a new mechanism for its occurrence [2]. The present authors [3] and also Wolf and Maret [4] found enhanced backscattering in their search for Anderson localisation of light. Anderson localisation is localisation due to randomness [5]. If the mean free path λ_{mf} in the random medium is shorter than some critical length λ_{cr}, the diffusion constant vanishes due to interference and we have (strong) localisation. Until recently, all studies concerned the localisation of *scalar* waves. Localisation of light is of particular interest because the *vector* character of electromagnetic waves introduces new aspects.

In order to observe strong localisation, λ_{mf} should be extremely short, but even if λ_{mf} is not short enough to make the diffusion constant vanish, one may still see interference effects: waves travelling the same light path in opposite directions (figure 1(*a*)) will emerge with the same phase in the 180° direction. If observed at an angle θ with this direction, their relative phase shift will be $(2r/\lambda)\cos(\alpha - \theta/2)\sin(\theta/2)$. The inset of figure 1(*a*) shows the intensity due to the time-reversed pair as a function of θ. Adding the patterns of many time-reversed pairs yields a constant 'background' with a narrow cone of enhanced intensity around the 180° direction (where all interference is constructive). The enhanced backscattering implies an increased probability of return for waves propagating in the medium and hence reduces the diffusion constant. This phenomenon is a precursor of (strong) localisation and is known as weak localisation. The present paper deals with manifestations of the vector wave character in the weak localisation of light.

The importance of polarisation as a parameter is illustrated in figure 1(*b*). The incident wave propagates in the direction perpendicular to the plane of the drawing and is vertically polarised. The polarisation vectors of the waves that are backscattered via the 'light paths' 1–2–3 and 3–2–1 are $\boldsymbol{P}^+$ and $\boldsymbol{P}^-$ respectively. It is seen that the polarised components $(\boldsymbol{P}^+)_\parallel$ and $(\boldsymbol{P}^-)_\parallel$ are equal, whereas the depolarised components $(\boldsymbol{P}^+)_\perp$ and $(\boldsymbol{P}^-)_\perp$ are not. Thus in the 180° direction there will

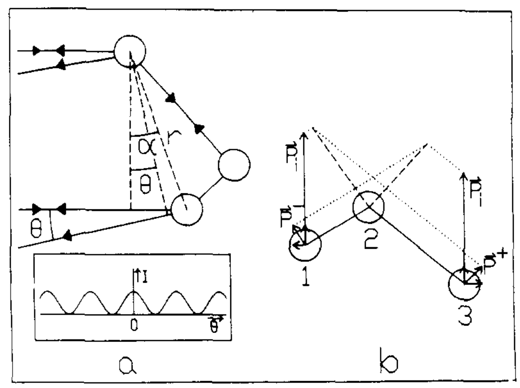

Figure 1. (*a*) Pair of time-reversed light paths. Inset: interference pattern of a time-reversed pair. (*b*) Light with polarisation vector $\boldsymbol{P}_i$ is incident in the direction perpendicular to the plane of the drawing. The components of $\boldsymbol{P}^+$ and $\boldsymbol{P}^-$ parallel to $\boldsymbol{P}_i$ are equal, whereas the perpendicular components are not.

0022-3727/88/100S28 + 04 $02.50

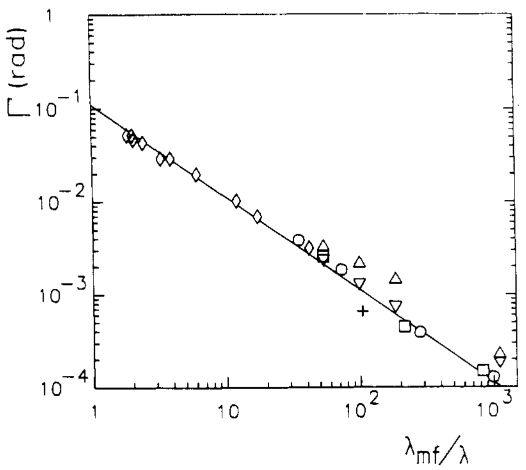

Figure 2. Width at 1.5 × background level (0.215 μm particle background corrected for single scattering), Γ, as a function of λ_{mf}: +, 2.02 μm polyvinyltoluene spheres in water; ○, 1,091 μm polystyrene spheres in water; □, 0.482 μm polystyrene spheres in water; ▽, 0.215 μm polystyrene spheres in water, scan $\|\boldsymbol{P}_i$ (note the abnormally large Γ values); △, 0.215 μm polystyrene spheres in water, scan $\perp\boldsymbol{P}_i$; ◇, ≈0.22 μm TiO_2 particles in 2-methyl-2,4-pentane-diol; full line, $\Gamma = 0.7\lambda/2\pi\lambda_{mf}$ (result from rigorous theory) [6].

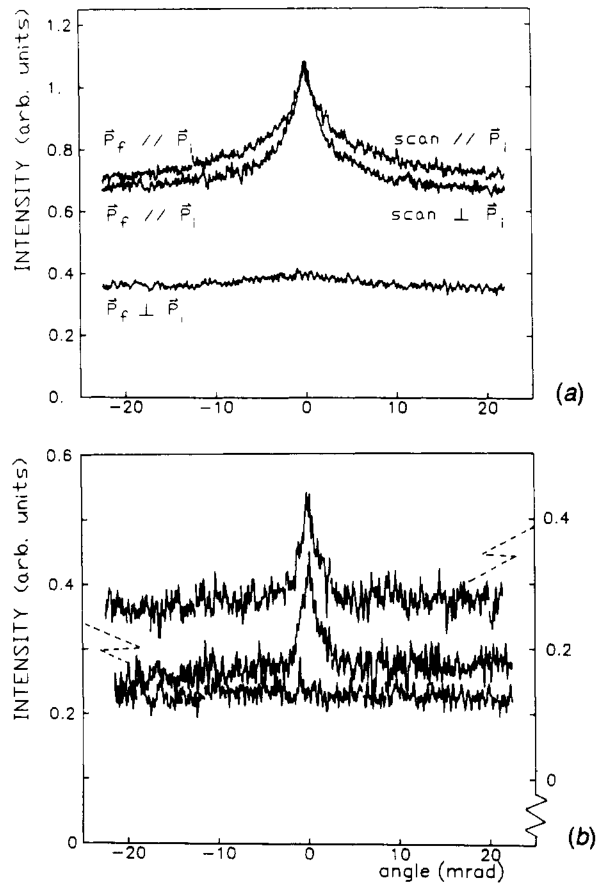

Figure 3. (*a*) Backscatter cones from a thick slab (2400 μm) of 9.6 vol% 0.215 μm polystyrene spheres in water: upper curve, polarised component, scan $\|\boldsymbol{P}_i$; middle curve, polarised component, scan $\perp\boldsymbol{P}_i$; lower curve, depolarised component (∥ and ⊥ scans coincide). (*b*) As for (*a*), but from the 'deep' slab between 60 and 2400 μm behind the interface of the sample.

be constructive interference (doubled intensity) in the polarised component, whereas in the depolarised component the interference depends on the geometry of the light path and may be anything from totally constructive to totally destructive. Thus one would expect enhancement factors slightly lower than 2 for the polarised component (the single-scattering contribution to backscattering has no interference term) and near 1 for the depolarised component. The cones of enhanced backscattering are made up of contributions of many time-reversed pairs, all having different geometries and different values for the displacement r. Since r scales with λ_{mf}, the width of the cone will relate to λ/λ_{mf}, where λ is the wavelength of the light. Figure 2 shows the width Γ at 1.5 × background level of the polarised cone as a function of λ_{mf}. The inverse proportionality demonstrates that the backscattering enhancement is indeed a result of interference.

The relative importance of the different orders of scattering depends on the phase function of the scatterers, so the shape of the cone may depend on, for example, particle size: 0.215 μm sphere samples, for instance, yield backscattering cones that are anisotropic, being broader in one direction than expected on the basis of λ_{mf} (figure 2). Intensity profiles recorded for the polarised and depolarised components of the light backscattered from a thick 9.6 vol% sample of 0.215 μm polystyrene spheres in water are shown in figure 3(*a*). The lower curve corresponds to the depolarised component, while the upper and middle curves correspond to the polarised component scanned parallel and perpendicular to the direction of incident polarisation respectively. It is seen that the background backscattered light is partially polarised, the intensity profile for the polarised component is spatially anisotropic, and the enhancement factor $I_{top}/I_{background}$ is somewhat less than 2 for the polarised component and slightly larger than 1 for the depolarised component. The curves in figure 3(*b*) were obtained by subtracting intensity profiles recorded for a thin sample from those of the thick sample. Thus the contributions from short light paths that never enter the 'deep' part of the thick sample cancel out, and what remains is the contribution of light paths long enough to have passed through this deep part. Comparing the curves associated with long light paths, we see that the background polarisation is now almost completely scrambled, the intensity profile of the polarised component is isotropic, and no enhancement is left in the depolarised component. It follows that the three polarisation effects are due to lower-order scattering. Figure 4 shows data corresponding to those of figure 3(*a*) but recorded using a 1500 μm sample of 9.6 vol% 1.091 μm spheres. The background polarisation is nearly completely scrambled, and no spatial anisotropy is seen in the polarised cone. On the other hand the enhancement in the depolarised component is more pronounced here.

A lot of theoretical work has already been done to explain the shape and width of the backscatter cone,

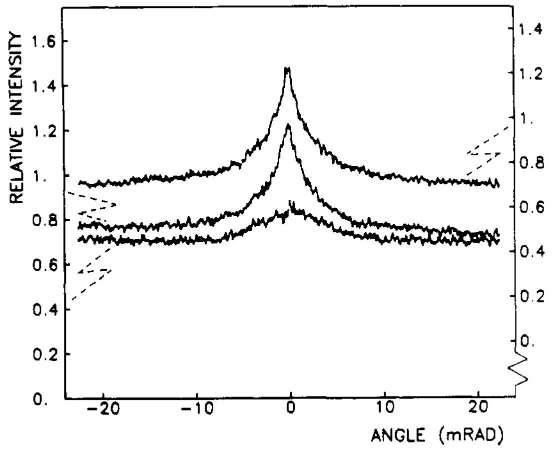

Figure 4. Backscatter cones from a 1500 μm slab of 9.6 vol% 1.091 μm polystyrene spheres in water: lower curve, depolarised component; middle curve, polarised component, scan $\perp \boldsymbol{P}_i$; upper curve, polarised component, scan $\parallel \boldsymbol{P}_i$.

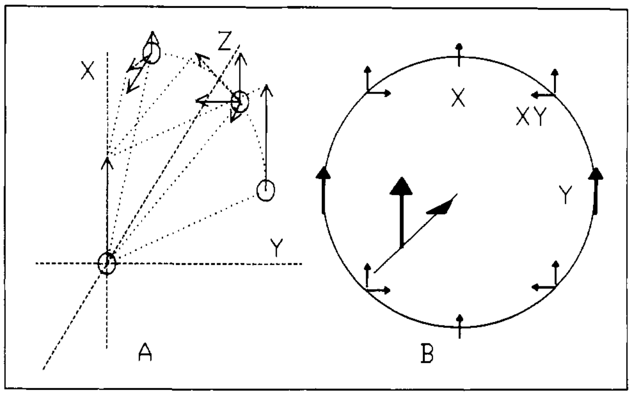

Figure 5. (*a*) Three second-order light paths for Rayleigh scattering. (*b*) Direction and amplitude of the backscattered wave in second-order Rayleigh scattering as a function of the relative orientation of the scattering particles.

and much of this work concerns the isotropic scattering of scalar waves. A rigorous theory [2, 6] and diffusion approximations [6–8] have been developed. The shape and width of the backscatter cone predicted by these scalar theories agree quite accurately with those found experimentally in the polarised light component for all but the smallest scatterers, but scalar theory cannot be used to describe the depolarised component.

In other work the vector character has been considered. We calculated the enhancement factor for the depolarised component for multiple Rayleigh scattering [9], and a diffusion theory for point-dipole scattering has been developed [10] which correctly predicts the partial retention of polarisation and the weak enhancement in the depolarised component, but not the spatial anisotropy in the polarised cone.

We will now present qualitative explanations in terms of the symmetry of the phase functions of the scattering particles for the observed vector character effects. Since these effects originate from low-order multiple-scattering processes, we will discuss them on the basis of properties of the very lowest-order processes that contribute significantly to the backscattering.

For the small-particle case we will assume Rayleigh scattering. In this case the second-order contribution to enhanced backscattering is larger than that of any other individual order. In a second-order process there is only one plane of scattering and therefore the interference between time-reversed waves is constructive in both the polarised and depolarised components (figure 5(*a*)). Figure 5(*b*) represents a part of the air–sample interface; x-polarised light is incident in the z direction. The directions of polarisation and the relative amplitudes of waves scattered via a first particle somewhere at the negative z axis and a second particle somewhere behind the interface areas marked x, y and xy are represented by vectors.

In the Mie case the power scattered by a particle is almost completely confined to a cone in the forward direction, the apex angle θ of which decreases with increasing size of that particle. As a consequence, light paths including scattering angles $>\theta$ will contribute very little. The very lowest-order light paths that do contribute significantly to the backscattering are therefore essentially coplanar configurations of π/θ scatterers (figure 6(*a*)). Figure 6(*b*) shows the large-scatterer limit for the direction of polarisation and the relative amplitude of a scattered wave as a function of the relative orientation of the two ends of a lowest-order light path. Since within the narrow cone of forward scattering associated with larger particles the amplitude of the scattered wave is practically independent of the angle φ between the incident polarisation and the normal to the plane of scattering, the x, y and xy processes are equally efficient in this limit.

From figures 5(*b*) and 6(*b*) the vector character effects are easily understood.

(1) The partial retention of polarisation found for small-particle samples occurs because in this case much of the original polarisation survives low-order scattering processes. In large-particle samples even the

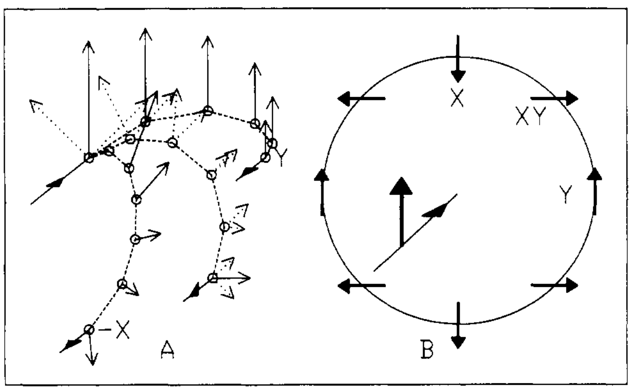

Figure 6. (*a*) Three 'lowest-order' light paths in (large-particle) Mie scattering. (*b*) Direction and amplitude of the backscattering wave as a function of the orientation of the 'shortest' light path in Mie scattering.

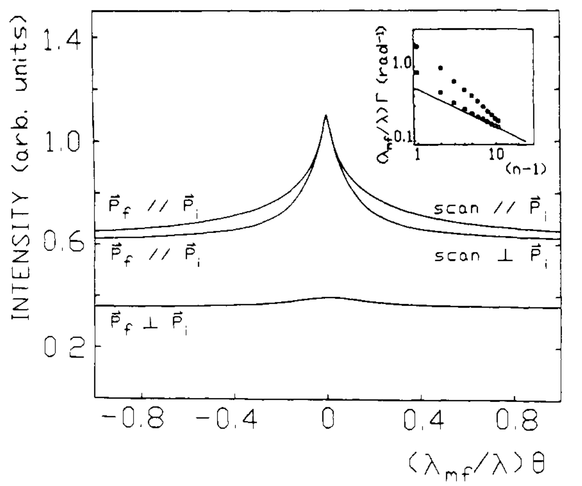

Figure 7. Simulated backscatter cones for multiple Rayleigh scattering; attribution of curves as in figure 3. Inset: Γ for the polarised component as a function of the order of scattering; upper series, scan $\| \boldsymbol{P}_i$; lower series, scan $\perp \boldsymbol{P}_i$; full line, $\Gamma = (0.5\lambda/\lambda_{mf})(n-1)^{-1/2}$, where n is the order.

lowest-order light paths that contribute to an important extent completely scramble the polarisation.

(2) The spatial anisotropy found in the polarised cone of small-particle samples results from the circumstance that the separation between both ends of the average polarisation-preserving light path is larger in the y direction than in the x direction. On average, the two-point-source interference patterns that constitute the cone are therefore broader in the x than in the y direction. In the large-particle limit this anisotropy does not occur (figure 6(b)).

(3) Enhancement in the depolarised component will occur if constructive interference between the depolarised components of time-reversed pairs of waves outweighs destructive interference. In both the small- and large-particle limits we find that in the lowest-order light paths the scattering centres are in a coplanar configuration and therefore the polarisation vectors of the time-reversed waves are parallel. With increasing order the light paths may assume more arbitrary shapes, and in the depolarised component destructive interference will become increasingly important, until in the high-order limit it balances constructive interference. Because of the low-order contributions, a net excess of constructive interference (and hence enhancement) in the depolarised component will occur in both the small- and large-particle limits, in contrast to the partial retention of polarisation and anisotropy, which only occur in the small-particle limit.

Our interpretation is confirmed by the results of a computer simulation of enhanced backscattering from a medium containing randomly distributed Rayleigh scatterers [9]. These results are presented in figure 7 and show clearly the three vector effects. An analogous simulation for large-particle scattering is possible in principle but would require an excessive amount of computing time.

Acknowledgment

This work is part of the research programme of the 'Stichting voor Fundamenteel Ondezoek der Materie' (FOM), which is supported financially by the 'Nederlandse Organisatie voor Wetenschappelijk Onderzoek' (NWO).

References

[1] Trowbridge T S 1984 *J. Opt. Soc. Am.* A **1** 831
[2] Tsang L and Ishimaru A 1985 *J. Opt. Soc. Am.* A **2** 2187
[3] van Albada MP and Lagendijk A 1985 *Phys. Rev. Lett.* **55** 2692
[4] Wolf P E and Maret G 1985 *Phys. Rev. Lett.* **55** 2696
[5] Anderson P W 1958 *Phys. Rev.* **109** 1492
Souillard B 1984 *Phys. Rep.* **103** 41
[6] van der Mark M B, van Albada M P and Lagendijk A 1988 *Phys. Rev.* B **37** 3575
[7] Akkermans E and Maynard R 1985 *J. Physique Lett.* **45** 1045
[8] Akkermans E, Wolf P E, Maynard R and Maret G 1988 *J. Physique* **49** 77
[9] van Albada M P and Lagendijk A 1987 *Phys. Rev.* B **36** 2353
[10] Stephen M J and Cwillich G 1986 *Phys. Rev.* B **34** 7564